Biosensors and Bioelectronics 68 (2015) 163–167

Contents lists available at ScienceDirect

Biosensors and Bioelectronics

journal homepage: www.elsevier.com/locate/bios

# Graphene oxide nanoribbon-based sensors for the simultaneous bio-electrochemical enantiomeric resolution and analysis of amino acid biomarkers

Aída Martín [a], Pilar Batalla [a], Javier Hernández-Ferrer [b], María Teresa Martínez [b], Alberto Escarpa [a,*]

[a] Departament of Anlytical Chemistry, Physical Chemistry and Chemical Engineering University of Alcalá, E-28871 Alcalá de Henares, Madrid, Spain
[b] Instituto de Carboquímica ICB-CSIC, Miguel Luesma Castán, 4, 50018 Zaragoza, Spain

ARTICLE INFO

*Article history:*
Received 6 September 2014
Received in revised form
9 December 2014
Accepted 11 December 2014
Available online 12 December 2014

*Keywords:*
Graphene nanoribbons
Amino acid
Bio-enantiomeric resolution

ABSTRACT

In this work, a straightforward in-situ measurement of L and D-amino acids (AAs) has been developed using disposable graphene oxide nanoribbon (GON) screen printed electrodes. For that, we took advantage of the electroactivity of certain clinically relevant AAs, such as tyrosine (Tyr) and methionine (Met), which are involved in important bacterial diseases (*Bacillus subtilis* and *Vibrio cholera,* respectively). The strategy is based on a dual electrochemical and enzymatic approach. The D-AA with the class enzyme D amino acid oxidase (DAAO) generates $H_2O_2$. This $H_2O_2$ is simultaneously detected with the L-AA, electroactive molecule by differential pulse voltammetry (DPV).

These GON disposable platforms use just 50 μL of sample and a total analysis time of 360 s. Both L and D enantiomers calibration and quantitative analysis were explored and were simultaneously detected with accuracy and precision in urine samples. Any interference of uric acid and other electroactive AAs was noticed.

This proposed electrochemical GON-based enantiomeric bio-sensor becomes a highly promising tool as future point of care for fast and reliable early diagnosis of diseases related to the presence of D-AAs.


## 1. Introduction

The analysis of enantiomeric (L,D) amino acids (AAs) has been an incessant problem for scientists, because of their same physical and chemical properties. Although L-AAs have been the most studied enantiomer since they are involved in important physiological functions, D-AAs have recently shown special interest in excellent literature. As selected and relevant example, Lam and collaborators described how in *Vibrio cholerae*, a racemase produces D-Methionine (D-Met), whereas in *Bacillus subtilis* generates D-Tyrosine (D-Tyr) (Lam et al., 2009). These unusual D-AAs, which could be considered biomarkers of important diseases, appear to modulate the synthesis of peptidoglycan, a strong and elastic polymer that is a component of the bacterial cell wall (Siegrist et al., 2013). Likewise, D-Tyr has been recognized as an important biomarker, because its excess in plasma and in urine indicates the presence of renal failures in humans (Young et al., 1994).

For the D,L-Tyr determination, there are several methods based on gas chromatography coupled with mass-spectrometry (GC–MS), high-performance liquid chromatography (HPLC) or capillary electrophoresis (CE) (Bruckner and Schieber, 2001; Kitagawa and Otsuka, 2011; Tojo et al., 2012). However, the high cost of both equipments and assays, the high time consumption and the use of derivatized AAs have avoided its application to directly monitor in situ measurements as point of care (POC) testing tools. Other approaches such as microchip electrophoresis (Huang et al., 2011), molecular imprinted polymers (MIPs) (Liang et al., 2005) or complex strategies based on inclusion complexes for the resolution of D,L amino acids (Tao et al., 2014) have also been explored with high sensitivity. However, these techniques still require specific expensive technology and qualified training.

Considering the clinical relevance of this issue, this work proposes a fast, simple and reliable in situ approach for the simultaneous resolution and determination of the target D,L-AAs on disposable electrochemical (bio-)sensors. The strategy involves the simultaneous enantiomeric resolution and determination of both (i) the D-AA bio-sensing using a class-enzyme that selectively reacts with one of the enantiomers to yield hydrogen peroxide and, (ii) the direct electrochemical sensing of the L-enantiomer, taking advantage of its inherent electroactivity, using a suitable

* Corresponding author. Fax: +34 91 885 49 71.
*E-mail address:* alberto.escarpa@uah.es (A. Escarpa).

http://dx.doi.org/10.1016/j.bios.2014.12.030
0956-5663/

graphene-based transducer. This strategy was applied to the simultaneous analysis of D and L Tyr and Met, as relevant target clinical AAs.

On the one hand, to assess the selectivity in the detection of the D-enantiomer biomarker as well as the complete quantitative reaction to hydrogen peroxide, we have used the enzyme D-amino acid oxidase (DAAO). This enzyme oxidatively deaminates D-AAs to the corresponding α-keto acids, without reacting with the corresponding L-AA.

On the other hand, the electrochemical sensing of the L-AAs needs to be selectively detected from the hydrogen peroxide, which is generated by the enzymatic reaction, with enough sensitivity and preventing the fouling. In this work, we introduce graphene to enhance these analytical requirements for the direct, selective and in situ electrochemical detection of the L-AAs involved in the racemic solution.

Graphene is a two dimensional net of carbon atoms bonded by $sp^2$ hybridization with extraordinary properties (Novoselov et al., 2004; Park and Ruoff, 2009; Lee et al., 2008), such as high surface area, excellent thermal and electrical conductivities, optical transparency, high mechanical strength and high elasticity, among others. However, beyond all their properties, its large surface area and high electrical conductivity have been interestingly exploited for sensing and biosensing purposes. Graphene family includes depending on the synthesis and applications a variety of different terms and structures (Martín and Escarpa, 2014). In this context, graphene nanoribbons (GNR) cover those synthesized by a controlled opening process or "unzipping" of carbon nanotubes (CNTs) (Terrones, 2009; Stankovich et al., 2006).

GNRs, fundamentally obtained by chemical oxidation of CNTs, are a really promising group of graphenes because they present very rich edge chemistry compared to pristine graphene. While pristine graphene has an inert chemical surface, the edges in GNR structure present functional groups which increase the reactivity and improve the electrochemical responses. The reactivity is mainly caused by the adsorption of analytes via π–π stacking interaction, with the non-oxydized benzene groups as well as, by electrostatic or hydrogen bond-based interactions with functional moieties located at the edges (Zhang et al., 2011). Despite the large and excellent analytical literature about graphene synthesized from graphite in electrochemical applications (Pumera et al., 2010; Shao et al., 2010; Kuila et al., 2011; Li and Xia, 2012), GNRs have not been so deeply studied as other graphenes in electrochemical applications (Martín and Escarpa, 2014). Herein, we hypothesize that the very rich edge chemistry of GNRs as well as the features derived from their high specific surface area such as electro-catalysis, enhanced sensitivity and their resistance-to-fouling offer us a suitable electrochemistry in this (bio)-sensing approach.

Despite the large number of applications employing DAAO to exclusively measure the generated $H_2O_2$ from the D-AAs by different electrochemical approaches (Lata and Pundir, 2013; Lata et al., 2013; Nieh et al., 2013; Sacchi et al., 2012; Wcislo et al., 2007; Wu et al., 2004; Dominguez et al., 2001) as far as we know, no examples of this enzyme coupled with graphene are found in the literature.

In sum, all these advantages of GNRs, in combination with the selectivity and sensitivity derived from the DAAO could constitute and excellent tool for the fabrication of highly specific sensors for enantiomeric analysis as simplified valuable alternative to the well-established technology in the field.

## 2. Materials and methods

### 2.1. Reagents, standards and samples

D-Tyrosine, L-tyrosine and L-methionine were purchased from Fluka Chemika (Buchs, UK) and hydrogen peroxide and D-methionine was obtained in Sigma Aldrich (St. Louis, MO, USA). Sodium dihydrogen phosphate was purchased from Panreac, (Badalona, Spain). D-Amino acid oxidase was purchased from Sigma Aldrich (St. Louis, MO, USA). All solutions were daily prepared using ultrapure water treated in a Milli-Q system (Millipore, Bedford, MA, USA). Urine samples 1:50 diluted were recollected from healthy individuals.

### 2.2. Apparatus and measurements

Field emission scanning electron microscopy (FE-SEM) micrographs were obtained on a JEOL Model JSM6335F equipment working at 5 kV. Direct determination of oxygen was carried out with a Flash 1112 analyzer from Thermo Fisher Scientific.

All electrochemical measurements were performed, at room temperature, on an USB-based portable electrochemical station μ-Stat 100 potentiostat controlled by PSLite 1.6 software and on a carbon screen-printed electrode (CSPE), which integrates the three-electrode system, a carbon working electrode of 4 mm diameter as well as a carbon counter and silver reference electrodes (Dropsens, Oviedo, Spain).

### 2.3. Preparation of graphene modified electrode

Graphene detailed synthesis and characterization features have been previously reported (Martín et al., 2014). In brief, graphene materials were synthesized from multiwall carbon nanotubes (MWCNTs) via the longitudinal unzipping method (Kosynkin et al., 2009). Using these oxidized nanoribbons (44 wt% oxygen content, 0.8 nm height by AFM, 46% C=O, 26% C–O, 19% $Csp^3$, 2% $Csp^2$ by XPS), reduced graphene oxide nanoribbons (14 wt% oxygen content, 1.2 nm height by AFM, 15% C=O, 10% C–O, 47% $Csp^2$, 10% $Csp^3$) were obtained by chemical reduction with $N_2H_4/NH_3$ (Gao et al., 2010).

Graphene oxide nanoribbons (GON) were dispersed to obtain a 0.5 mg $mL^{-1}$ sample in water by ultrasonication in a bath for 30 min. Graphene reduced nanoribbons (GRN) were dispersed to obtain a 0.5 mg $mL^{-1}$ dispersion in water/$NH_3$ (1% v/v) by ultrasonication in a bath for 30 min, followed by tip sonication using a VCX130, (Sonics, Newtown, USA) for 2 min at 130 W. The graphene nanoribbons modified electrodes were prepared by casting 10 μL of 0.5 mg $mL^{-1}$ graphene nanoribbons on the CSPE surface. This volume was previously optimized by modifying the CSPE with different volumes 5, 10, 15 and 20 μL of 0.5 mg $mL^{-1}$ and exploring its electrochemical behavior by cyclic voltammetry with 0.5 mM $K_3Fe(CN)_6$ in 1 M KCl on both graphene surfaces. The modified CSPEs will be named GON and GRN along this work.

### 2.4. Analytical procedure

Different concentrations and mixtures of D and L-tyrosine were prepared in sodium dihydrogen phosphate buffer adjusted with NaOH. The enzyme was also diluted in the same buffer. Both pH value and buffer concentration were optimized, as well as the enzyme concentration.

Following the optimal reaction conditions, 25 μL of a 0.50 mg $mL^{-1}$ DAAO in 10 mM $NaH_2PO_4$ pH 7 was placed on the electrode. Immediately, 25 μL of the AA solution in 10 mM $NaH_2PO_4$ pH 7.0 was added, considering this time reaction 0 s. These total 50 μL of the solution permitted to cover the three

electrode electrochemical cell and to record the measurements.

After the optimized reaction time, differential pulse voltammetry (DPV) was scanned. DPV was performed with a potential range between +0.20 to +1.20 V and +0.30 to +1.50 V for Tyr and Met analysis, respectively, with 5 mV step potential, 25 mV pulse potential, 5 mV $s^{-1}$ scan rate, 0.07 s pulse time and 3 s equilibration time.

## 3. Results and discussion

### 3.1. Strategy for the enantiomeric amino acid analysis

The proposed strategy involves both the simultaneous D-AA bio-sensing, using a class-enzyme that selectively reacts with D-enantiomer to yield hydrogen peroxide, and the direct electrochemical sensing of the L-enantiomer using GNR transducers. This strategy was applied to relevant AAs such as Tyr and Met, as it is illustrated in Fig. 1, on a disposable platform, just consuming 50 µL of sample and avoiding any adsorption or covalent union of the enzyme. Under optimum (bio-chemical) conditions (10 mM PBS pH=7.0), L,D-AA racemate was resolved under 360 s. Indeed, L-Tyr and L-Met were detected at +0.59 V and +1.25 V, respectively and the hydrogen peroxide was oxidized at +0.87 V on the GON. Suitable controls were also carefully checked. Background signal displayed by buffer and the blank of the enzyme without presence of D or L AA did not give any peak in the scanned window potential (see Fig. 1). No formation of hydrogen peroxide at the L-AA tested concentrations was either noticed.

### 3.2. Optimization of L-amino acid electrochemical sensing: optimizing graphene transduction

Two GNRs, graphene reduced nanoribbons (GRNs) and graphene oxide nanoribbons (GONs) were explored in order to examine the suitability of these two nanomaterials for the determination of the target enantiomers. As it is shown in Fig. 2, GNRs exhibited an improved electrochemical performance in comparison with non-modified CSPE. Both GNRs presented much higher current intensity and lower oxidation potentials than the non-modified CSPE. The marked electrocatalytic effect exhibited by these two graphene materials could be explained considering the interactions between both graphene structures and Tyr. The interactions are caused by the adsorption of analytes via π–π stacking interaction with the non-oxydized benzene groups, as well as by electrostatic or hydrogen bond-based interactions with functional moieties located at the edges. Considering the results obtained by X-ray photoelectron spectroscopy (XPS), GON showed

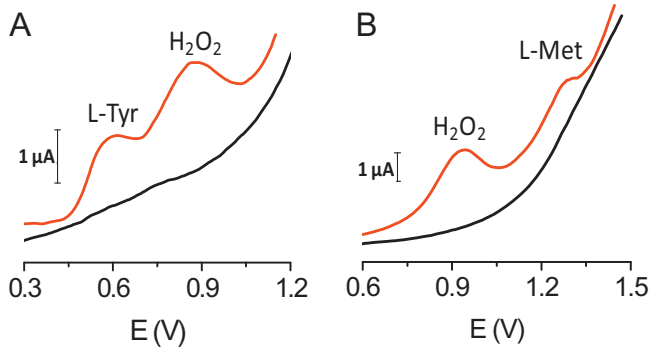


**Fig. 1.** Voltammograms for enantiomeric analysis of 1 mM L,D AAs: (A) Tyr and (B) Met in 10 mM PBS, pH=7.0, and 0.5 mg/mL DAAO after 360 s. Background signal of PBS with DAAO (black).

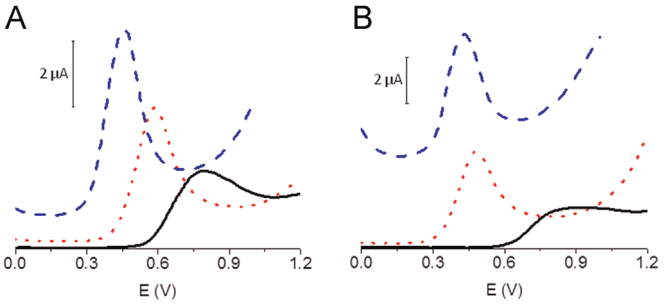


**Fig. 2.** Voltammograms for L-Tyr (A) and D-Tyr (B), using GRN (dashed blue), GON (dotted red) and non-modified CSPE (black) in 10 mM PBS, pH=7.0.

high percentage of carboxyl and alcohol groups while the content of $sp^2$ carbons and defects in the structure was increased in GRN (Martín et al., 2014).

Remarkably, both L and D Tyr showed the highest intensity current and the lowest oxidation potentials with GRN, however, at potentials over +0.50 V, in which analytes such as Met and $H_2O_2$ are oxidize, the background signal of GRN makes difficult the detection of molecules of high oxidation potential. In this case, in GRN, potentials over +0.50 V provokes the oxidation of the carbon material, avoiding the detection of $H_2O_2$. However, this phenomenon does not appear in GON, becoming this transducer the most suitable for the detection of both $H_2O_2$ and Met with improved performance than CSPE. Hence, GON becomes as the most suitable electrochemical transducer for D Tyr, Met and $H_2O_2$ detection. Furthermore, GON demonstrated to improve the sensitivity as well as simultaneously detect and resolve the target enantiomers in comparison with non-modified CSPE that did not achieve so good results. Table S1 lists the oxidation potentials and the amperometric currents obtained. Remarkably, as it listed in this table, in comparison with CSPE, these GON dramatically improved the reproducibility of the electrochemical sensing of the L,D-enantiomers (up to 20-folds i.e. from RSDs=19% in CSPE to RSDs=1% in GON, in amperometric currents, $n=5$). Overall, these results confirm our previous hypothesis regarding the electrocatalysis, high sensitivity and the anti-fouling effect expected from these carbon nanomaterials.

In order to elucidate how graphene is deposited on the electrode surface, FE-SEM images were obtained. In Fig. 3, clear differences were noticed in the surface of the electrode between the modified GON and non-modified CSPE (inset). Indeed, GON layers of several hundred of nm deposited on CSPE are randomly distributed along the electrode. They appear as thin GON curtains, creating a new surface.

### 3.3. Optimization of D-amino acid electrochemical biosensing: optimizing enzymatic reaction

The enzymatic reaction was directly performed in situ on the electrode surface with a 50 µL drop mixture of the racemic AA and DAAO, behaving the electrode surface as the reaction cell. In this approach, the enzyme is not covalently immobilized onto the electrodic surface, therefore, the procedure is simpler than in the most classical covalent-based approaches.

On the one hand, Table 1 lists the enzymatic reaction progress. While the D-Tyr current intensity peak decreases, the $H_2O_2$ generated in situ increases. The optimal reaction time was 360 s. At that time, D-Tyr was quantitatively consumed and consequently, the signal obtained is only from the generated hydrogen peroxide. These results indicated the accurate resolution of the racemate. We have also studied the buffer influence in the enzymatic reaction, varying both buffer concentration and pH values (results

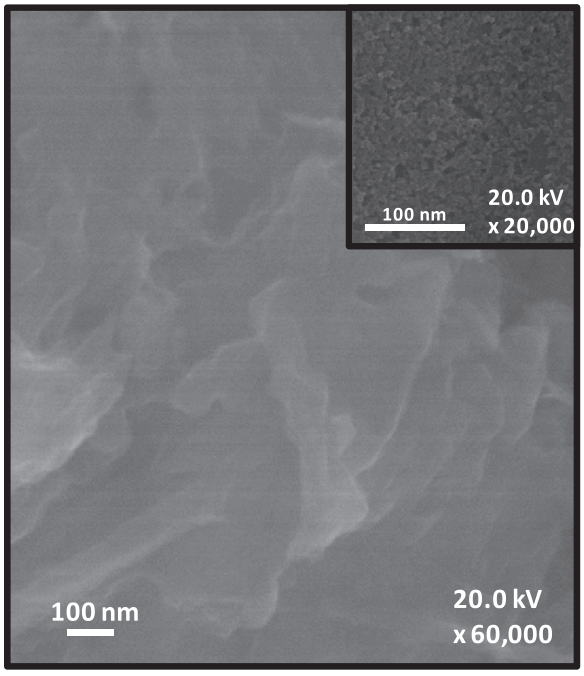


**Fig. 3.** Field-emission scanning microscopy images. Micrograph for modified GON and CSPE (inset) electrodic surfaces.

**Table 1**
Optimization of the enzymatic reaction time.

| Time (s) | | 0 | 60 | 120 | 180 | 240 | 300 | **360** | 420 |
|---|---|---|---|---|---|---|---|---|---|
| *I* (μA) | D-Tyr | 0.614 | 0.598 | 0.890 | 0.481 | 0.360 | 0.017 | ND | ND |
| | $H_2O_2$ | 0.574 | 0.636 | 0.733 | 0.780 | 0.848 | 0.855 | 0.927 | 0.932 |

1 mM D-Tyr and 0.5 mg $mL^{-1}$ DAAO in 10 mM $NaH_2PO_4$ pH 7.0.

showed in Tables S2 and S3). The buffer optimal conditions were 10 mM and pH 7.0 for $NaH_2PO_4$.

On the other hand, enzyme and substrate concentrations are also important values to be optimized. While L-Tyr showed no reaction with the enzyme, Fig. 4A shows the increase in the current intensity of the generated $H_2O_2$ and the decrease in the D-enantiomer when the enzyme concentration increased. At concentrations of DAAO higher than 0.50 mg/mL, the D-AA completely reacted with the enzyme, the intensity of the hydrogen peroxide kept constant and the correspondent intensity of the D-AA was zero. Therefore, this value was considered the optimal enzyme concentration. Moreover, Fig. 4B suggests that at concentrations higher than 1.0 mM of substrate, the linearity in the $H_2O_2$ intensity

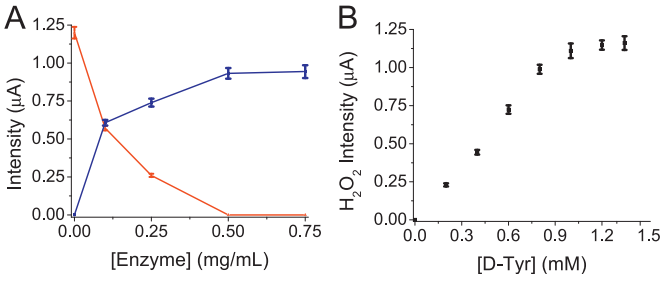


**Fig. 4.** (A) Plot of current intensities for extinction of D-Tyr (red) and apparition of enzymatic product, $H_2O_2$ (blue) versus enzyme concentration for 1 mM D-Tyr 10 mM PBS, pH=7 after 360 s. (B) Plot representation of generated hydrogen peroxide current intensity versus D-Tyr concentration for 1 mM D-Tyr in 10 mM PBS, pH=7.0 and 0.5 mg/mL DAAO after 360 s. Bar errors for %RSDs ($n$=3). (For interpretation of the references to color in this figure legend, the reader is referred to the web version of this article.)

is lost and the enzyme is saturated by the substrate. The good response of the enzyme and these results demonstrated that the enzymatic reaction carried out in the drop solution was perfectly working in the optimized conditions. Furthermore, the strategy could be developed in just 50 μL of sample without any covalent immobilization bond of the enzyme on the electrodic surface.

Under these electrochemical and bio-sensing optimized conditions, a careful study of precision of the method was performed. The electrochemical graphene-based enantiomeric bio-sensor presented excellent intra-electrode repeatability (RSD ≤ 3% for redox potentials and RSD ≤ 4% for intensity currents, $n$=5) and inter-electrode reproducibility (RSD ≤ 5% for redox potentials and ≤ 10% for intensity currents, $n$=5). It indicated an excellent performance of the electrode to be used as a further disposable platform.

### 3.4. Simultaneous calibration and analysis of the enantiomers

The objective of this paper is the development of an electrochemical point of care system capable of detecting and resolving the D-AA, in a similar concentration range than the one established by Lam et al. (2009). Consequently, the simultaneous enantiomeric calibration was also another feature assayed during the evaluation of the sensor performances. Interestingly, Fig. 5A shows the DPV for different L,D Tyr concentrations, therefore, the two peaks increase with the AAs concentration, one of the peaks around +0.61 V corresponding to L-Tyr and the other around +0.92 V from $H_2O_2$ generated from D-Tyr at each assayed concentration. The calibration plots (see Fig. 5B) showed excellent linearity with ($R^2 \geq 0.990$) and low LODs of 100 and 60 μM for L and D Tyr, respectively.

In order to evaluate this strategy we chose urine samples since D-Tyr is a renal biomarker (Young et al., 1994). Furthermore, due to the health hazard of working with bacteria, urine samples become a suitable matrix to assess future diagnosis using these samples as non-invasive and more accessible ones.

Fig. 5C shows the overall analysis carried out using healthy urine samples. Firstly, as expected, no detection of D-Tyr was noticed, however, uric acid (UA) was identified at +0.32 V in both non-spiked (voltammogram black) and spiked urine samples (voltammogram blue) releasing quantitative and reproducible recoveries of 100 ± 1%. Secondly, spiked urine samples in Tyr enantiomers were also assayed (voltammogram red) obtaining quantitative and reproducible recoveries of 95 ± 5% and 99 ± 3% ($n$=3) for L-Tyr (at +0.64 V) and generated $H_2O_2$ (at +0.99 V), respectively.

Overall, L and D Tyr enantiomers were determined with accuracy and precision in presence of UA, giving an additional value to the proposed approach. Even, under these conditions, the simultaneous detection of the two targeted D-AAs towards the confirmation of the detection of the L-AAs (Tyr and Met) could be possible.

The influence of other amino acids for the analysis of complex samples is expected, therefore, as well as L-Met, L-Histidine (L-His) was also considered as potential electroactive AA interference in biological fluids. This AA did not interfere in the Tyr analysis because its oxidation potential was found over the ones for tyrosine and hydrogen peroxide. Also, the presence of DAAO did not give any further signal, indicating the selectivity of the enzyme to D-enantiomers exclusively.

The analysis of D-Tyr in urine samples was successfully performed in less time and with low cost, in comparison with other approaches found in the literature. The results obtained in this preliminary application are very valuable and promising. They have allowed the selective detection of the target D-AAs studied in this work (D-Met and D-Tyr), involved in important bacterial diseases (*V. cholerae* and *B. subtilis*), and they have also given a reliable and selective assessment of a D-AA index towards the electrocatalyzed detection of hydrogen peroxide. The successful exploration of these target D-AAs in non-invasive urine samples

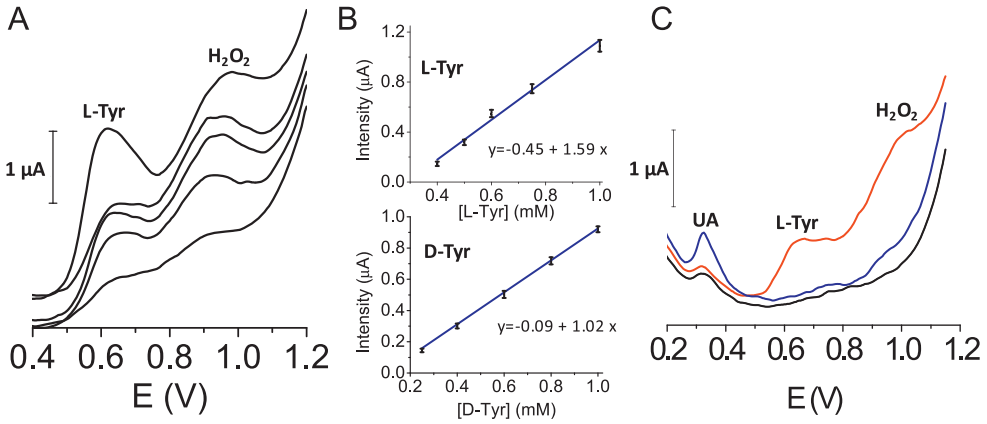


**Fig. 5.** (A) Voltammograms from 0.25 mM to 1.25 mM of D and L-Tyr. (B) Linear plot and linear equation for L (up) and D-Tyr (down), respectively. Bar errors for %RSDs ($n=3$). (C) Voltammograms obtained for urine analysis. Diluted urine (black), fortified with 1 mM UA (blue) and fortified with 0.50 mM D-Tyr and L-Tyr (red). Other conditions see Section 2. (For interpretation of the references to color in this figure legend, the reader is referred to the web version of this article.)

opens an exciting perspective for rapid in-situ diagnosis.

## 4. Conclusions

The strategically driven selectivity of the D-AAO towards D-AAs and the inherent electrocatalysis, sensitivity and anti-fouling exhibited by GON to L-AAs and hydrogen peroxide generated from D-AA have allowed to resolve the racemic mixture of L and D electroactive target AAs with clinical relevance such as Tyr and Met.

The disposable electrochemical graphene-based enantiomeric biosensor allows a fast, selective, accurate and reproducible determination of D-Tyr and D-Met biomarkers in urine samples in 360 s and using just 25 µL of sample exploiting the advantages of the enzyme in solution avoiding any covalent immobilization bond of the enzyme on the electrodic surface.

From a technical point of view, the possibility of simultaneously detect these enantiomers and uric acid without any separation step is of chief interest for clinical field since the equipment used is portable, adaptable in any electronic equipment and easy to use by any minimally trained personnel.

It is worth to notice that this work opens the possibility of using this strategy for new enantiomeric resolution of molecules. Additionally, although this work has been merely focused on the resolution of L and D AAs, this work opens the possibility of measuring total D AA content (D-AA Index, even for non-electroactive amino acids). This new suggestion could be interesting to assure the presence of certain diseases or malfunctions in biological samples becoming a valuable screening tool for diagnosis. Even, this approach becomes highly promising as future point of care for fast in situ early diagnosis of these diseases related to the presence of D-AAs.

## Acknowledgements

The authors gratefully acknowledge the financial support from the Spanish Ministry of Science and Innovation projects CTQ2011-28135, TEC2010-15736, PRI-PIBAR-2011-1 and from the NANOAVANSENS program from the Community of Madrid (S2013/MIT-3029). Dra. Batalla acknowledges the program AVANSENS (P2009/PPQ-1642) for her post-doctoral contract. A. Martin acknowledges the FPU fellowship received from the Ministry of Education, Culture and Sports.

## Appendix A. Supplementary material

Supplementary data associated with this article can be found in the online version at http://dx.doi.org/10.1016/j.bios.2014.12.030.

## References

Bruckner, H., Schieber, A., 2001. Biomed. Chromatogr. 15, 166–172.
Dominguez, R., Serra, B., Reviejo, A.J., Pingarron, J.M., 2001. Anal. Biochem. 298, 275–282.
Gao, X., Jang, J., Nagase, S., 2010. J. Phys. Chem. C 114, 832–842.
Huang, Y., Shi, M., Zhao, S., Liang, H., 2011. J. Chromatogr. B 879, 3203–3207.
Kitagawa, F., Otsuka, K., 2011. J. Chromatogr. B 879, 3078–3095.
Kosynkin, D.V., Higginbotham, A.L., Sinitskii, A., Lomeda, J.R., Dimiev, A., Price, B.K., Tour, J.M., 2009. Nature 458 (872-U5).
Kuila, T., Bose, S., Khanra, P., Mishra, A.K., Kim, N.H., Lee, J.H., 2011. Biosens. Bioelectron. 26, 4637–4648.
Lam, H., Oh, D.C., Cava, F., Takacs, C.N., Clardy, J., de Pedro, M.A., Waldor, M.K., 2009. Science 325 (5947), 1552–1555.
Lata, S., Batra, B., Kumar, P., Pundir, C.S., 2013. Anal. Biochem. 437, 1–9.
Lata, S., Pundir, C.S., 2013. Bioprocess Biosyst. Eng. 36, 81–89.
Lee, C., Wei, X., Kysar, J.W., Hone, J., 2008. Science 321, 385–388.
Li, Z.J., Xia, Q.F., 2012. Rev. Anal. Chem. 31, 57–81.
Liang, H.J., Ling, T.R., Rick, J.F., Chou, T.C., 2005. Anal. Chim. Acta 542, 83–89.
Martín, A., Hernández, J., Vázquez, L., Martínez, M.T., Escarpa, A., 2014. R. Soc. Chem. Adv. 4, 132–140.
Martín, A., Escarpa, A., 2014. Trends Anal. Chem. 56, 13–26.
Nieh, C., Kitazumi, Y., Shirai, O., Kano, K., 2013. Biosens. Bioelectron. 47, 350–355.
Novoselov, K.S., Geim, A.K., Morozov, S.V., Jiang, D., Zhang, Y., Dubonos, S.V., Grigorieva, I.V., Firsov, A.A., 2004. Science 306, 666–669.
Park, S., Ruoff, R.S., 2009. Nature Nanotechnol. 4, 217–224.
Pumera, M., Ambrosi, A., Bonanni, A., Chng, E.L.K., Poh, H.L., 2010. Trends Anal. Chem. 29, 954–965.
Sacchi, S., Rosini, E., Caldinelli, L., Pollegioni, L., 2012. Unnatural Amino Acids: Methods Protoc. 794, 313–324.
Shao, Y., Wang, J., Wu, H., Liu, J., Aksay, I.A., Lin, Y., 2010. Electroanalysis 22 (10), 1027–1036.
Siegrist, M.S., Whiteside, S., Jewett, J.C., Aditham, A., Cava, F., Bertozzi, C.R., 2013. ACS Chem. Biol. 8, 500–505.
Stankovich, S., Dikin, D.A., Dommett, G.H.B., Kohlhaas, K.M., Zimney, E.J., Stach, E.A., Piner, R.D., Nguyen, S.T., Ruoff, R.S., 2006. Nature 442, 282–286.
Tao, Y., Dai, J., Kong, Y., Sha, Y., 2014. Anal. Chem. 86, 2633–2639.
Terrones, M., 2009. Nature 458, 845–846.
Tojo, M., Murakami, M., Nagata, Y., 2012. J. Chromatogr. Sci. 50, 393–395.
Wcislo, M., Compagnone, D., Trojanowicz, M., 2007. Bioelectrochemistry 71, 91–98.
Wu, X.X., Van Wie, B.J., Kidwell, D.A., 2004. Biosens. Bioelectron. 20, 879–886.
Young, G.A., Kendall, S., Brownjohn, A.M., 1994. Amino Acids. 6, 283–293.
Zhang, S., Tang, S., Lei, J., Dong, H., Ju, H., 2011. J. Electroanal. Chem. 656, 285–288.